TRANSPORT PROBLEMS 2024 Volume 19 Issue 4
PROBLEMY TRANSPORTU DOI: 10.20858/tp.2024.19.4.08

Keywords: timing chain; engine; strength; quality; forces

Kazimierz WITASZEK[1]*, Zbigniew STANIK[2]

EVALUATION OF TIMING CHAIN QUALITY AND ITS EFFECT ON TIMING SYSTEM OPERATION

Summary. Internal combustion engines are still the main source of propulsion for automotive vehicles. The timing system plays a very important role in the proper functioning of these engines. One of the widely used technical solutions to drive this system is the timing chain. However, in recent years, there has been a clear trend towards more frequent timing system failures. Many research works have focused on wear analysis or finite element method (FEM) modeling of chains. In contrast, it was decided to carry out a comparative study of the mechanical properties of new timing chains that are commercially available as spare parts for automotive workshops. The present study was carried out on timing system components of the popular Multijet 1.3 diesel engine used in Fiat, Opel, and Suzuki vehicles. Force-elongation curves were obtained for each of the tested chains, allowing their elongation under load to be estimated. In addition, breaking forces were measured, and breaking mechanisms were analyzed to compare the quality of the chains. Numerical parameters were proposed to estimate the quality of the tested chains. The chain tensioning forces resulting from the operation of the hydraulic tensioner were also estimated. The effect of the dynamic forces stretching the chain elastically on the timing accuracy during engine operation was also calculated.

1. INTRODUCTION

One of the most important factors influencing vehicle operating costs and reliability is the amount and type of maintenance and repair work and the quality of spare parts used. Despite the widespread promotion of electromobility in transport, the vast majority of existing road vehicles are still equipped with conventional internal combustion engines.

The reliability of an engine is often determined by its basic components. These include the drive to the timing system, which can be implemented in one of three ways: by gear wheels, by a timing chain, or by a toothed belt. For most car engines, this can be a timing chain or timing belt. For heavy-duty engines in agricultural or construction machinery, gears are more likely to be used.

For many years, timing chains have often been a symbol of high durability and reliability. However, the trend of downsizing engines while increasing their power in order to meet the demands of continuous emission reduction is contributing to various engine failures [1] and reductions in their reliability and durability. Modern timing chain drives are subject to continuous development, and research is being carried out to improve their reliability [2]. However, there is a formidable competitor in the form of timing belts, the design of which is also undergoing intensive development [3]. Despite advances in technology, there has been a significant increase in the failure rate of timing systems on

[1] Silesian University of Technology, Faculty of Transport and Aviation Engineering; Krasińskiego 8, 40-019 Katowice, Poland; e-mail: kazimierz.witaszek@polsl.pl; orcid.org/0000-0002-3105-0532
[2] Silesian University of Technology, Faculty of Transport and Aviation Engineering; Krasińskiego 8, 40-019 Katowice, Poland; e-mail: Zbigniew.Stanik@polsl.pl; orcid.org/0000-0003-1965-4090
*Corresponding author. E-mail: kazimierz.witaszek@polsl.pl

certain engines in recent years. Historically, the timing chain, unlike the timing belt, has had a service life comparable to the overall life of the engine.

Over the last 10 years, it has become apparent that engine manufacturers have used various design solutions to reduce emissions, but this has not always been done with a focus on durability and reliability. For example, emission reductions can be achieved by reducing internal friction losses in the engine. The timing system can be responsible for up to 5–10% of total engine friction [4], so modern engines are also optimized to reduce friction losses. Older timing chain designs had significant energy losses due to friction. The results of a 2001 study presented in [5] estimated that total timing chain friction accounted for 16% of total engine friction. Significant progress has been made in recent years, and for newer engines, these losses are estimated to be less than 5% [6].

A further reduction in energy loss by reducing friction is possible by adjusting the chain tension. However, the introduction of the surface structuring of the elements according to the results presented in [7] did not reduce friction losses and could even increase them. The design of the modern, downsized turbocharged engine, which is primarily emissions-orientated, results in maximum cylinder pressures of 13 MPa for aggressive fuel economy concepts and as much as 20 MPa for high-performance variants [6]. These pressures are two to three times higher than those of naturally aspirated engines. Together with the use of dual VVT mechanisms, friction-optimized crankshafts with reduced bearing diameters, this results in a significant increase in dynamic loads [6]. Downsizing the engine by reducing the number of cylinders increases the dynamic load on the crankshaft while reducing the excitation frequency. The increased vibrations are transmitted to the timing system, further increasing the dynamic loads transmitted through its components.

In order to improve the reliability of highly loaded engines, dynamic analysis studies are carried out using numerical modeling. The analysis of the dynamics of timing systems is also one of the most frequently published research topics. The results of such works indicate a high variability of forces over time and high maximum values of the forces transmitted by the timing chain, which can exceed 1000 N for a two-chain sprocket system [8] and 2000 N for a chain operating with three sprockets [9]. The authors of [10] explicitly stated that the study of timing system dynamics is of paramount importance when designing an internal combustion engine. Unacceptable timing system dynamics ultimately lead to engine failure through incorrect valve timing, fuel injection, and unacceptable engine vibration levels. Despite the high dynamic loads on the timing system components in a properly designed engine, these do not exceed the critical values allowed for the chain. This is shown by the results published in [11].

Varying dynamic loads on components can cause them to vibrate. The vibration energy is transmitted through the air to the surroundings, resulting in noise, which is an undesirable effect. Therefore, research is being carried out to reduce engine noise, including that of the timing system. As a result, a so-called quiet chain has been developed, the dynamics of which have been modeled and experimentally verified in [12]. The results show, among other things, the occurrence of maximum tractive forces above 1200 N. A comprehensive analysis of the silent timing chain dynamics of the V12 engine, together with the optimization of the meshing angles, was published in [13]. The models were also verified experimentally. The results show that the optimization of the meshing angles reduces the chain stress from 2600 N to about 1700 N. The authors recommend this comprehensive approach for the analysis of chain drives of different types.

A useful computational tool for studying the dynamics of the timing chain can be the Fourier FFT analysis of the multibody dynamic simulation model [14]. The simulation resulted in chain tensile forces of 1200 N. The use of hydraulic chain tensioners helps reduce chain vibration as the tensioner elements act as a hydraulic damper. The behavior of the damper depends on the size of the leakage gap. Its correct selection is the key to achieving correct damping [15]. As a result of the mechanical loads involved and the phenomenon of friction during operation, chains and other components of the timing system are subject to wear. Chain wear is the main reason that the chain can no longer perform its function properly and must be replaced with a new one. In today's emissions-focused engines, reduced engine oil volume and extended oil change intervals, as well as high specific power, increase the accumulation of soot in the oil, which negatively affects the lubrication conditions for engine components, including the timing system [6]. Similarly, the use of low-viscosity oils affects the lubrication processes.

Therefore, the wear processes of valve train components are frequently researched, and the results are widely published in scientific journals. Wear experiments can be carried out on special test benches in a system that corresponds to the work of the components in the engine. To save energy, a recirculating power system can be used and two timing chains can be tested simultaneously [16]. Stands that test a specific friction pair, known as tribometers, are also often used. Depending on the test criteria adopted, they can operate in various geometric arrangements that reproduce tribological phenomena in real systems.

The wear of timing system components can also be mathematically modeled. A numerical model based on Fleischer's energetic wear equation can be used to predict the wear of a single-row timing chain, the results of which correlate with experimental tests on a real vehicle engine used for approximately 50,000 km, as published in [17]. A comprehensive review of methods for investigating and modeling timing chain wear was published in [18]. It was also noted that chain elongation occurs due to wear. The change in chain length has a direct impact on the accuracy of successive timing phases and fuel injection. Preliminary mathematical modeling of wear, followed by testing on tribotesters, can reduce the cost of designing new engines and the environmental impact.

In comparison to toothed belt-based drives, chain drives are known to be slightly noisier. In the context of the design of timing chain drives, an integrated approach can be employed in order to achieve optimal system design [19].

Cars are sold in a competitive free market. Failure mode and effects analysis (FMEA), one of the tools of concurrent engineering (CE), can be used to reduce the cost of introducing new solutions. It is widely used to identify and eliminate potential failures at the design and production stages. In this way, a faulty product is detected and eliminated at an early stage so that it does not reach the customer [20]. It is also advantageous to make use of numerical methods and mathematical modeling [21]. There have been reports of increased failure rates of timing systems, including those based on chain drive, from automotive service repair shops in recent years. Failure of the timing system of a modern internal combustion engine can lead to catastrophic engine failure [22]. As engine manufacturers seek to reduce the level of crankshaft torsional vibration [23], timing drive designs that are located on the clutch and gearbox side are being used. As such, the cost of repairing such an engine is increased by the need to remove it from the vehicle each time. Therefore, for certain failures, repair becomes financially unacceptable [24].

An analysis of the available literature showed that research topics describing the properties and quality of available spare parts for valve train systems, including chains, had not yet been investigated and published. Therefore, it was decided to carry out a comparative study of the mechanical properties of timing chains for the Multijet 1.3 engine. An innovative approach has also been used to calculate the effect of dynamic forces acting on the chain on the accuracy of timing during engine operation.

2. METHODOLOGY AND SCOPE OF THE RESEARCH

In recent years, there has been a concerning increase in the number of vehicle failures related to timing system failure. Unfortunately, engines fitted with timing chains are no exception. Undoubtedly, a major reason for this is the desire of engine manufacturers to reduce engine weight while increasing power. This results in high mechanical loads, which, combined with long engine oil change intervals, harm the durability of the drive units. At the same time, many independent manufacturers offer their products as spare parts to be used during engine service. Information gathered from service garages indicates that the quality of spare parts available on the market varies greatly. Therefore, it was decided to carry out a study to investigate the influence of the quality of commercially available timing chains on the operation of the timing system.

The methodology and scope of the study are shown in Fig. 1. Chains designed for the popular 1.3 Multijet turbocharged diesel engines were tested. These engines were used in several Fiat, Opel, and also Suzuki car models. After removal from their transport packaging, the chains were subjected to the first part of the macroscopic examination. They were photographed, and their appearance, distinctive marks, and condition on delivery were evaluated. The chains were then subjected to a static tensile test to determine their deformation under load. The stretching of the chains started with a range of relatively low forces that might occur during engine operation.

The force was then increased well beyond the levels encountered in the engine until the chain broke. This range was investigated in order to obtain results to compare the strength of the chains and their mechanical performance. The specimens destroyed during the static tensile test were again subjected to macroscopic and microscopic examination. The appearance of the chain fracture points made it possible to identify the mechanisms of loss of cohesion and the weakest points. The microstructure of the chain elements was studied to verify that they were all manufactured similarly. Strength parameters, together with information on failure mechanisms and microstructural information, were used for comparing the quality of commercially available chains as spare parts.

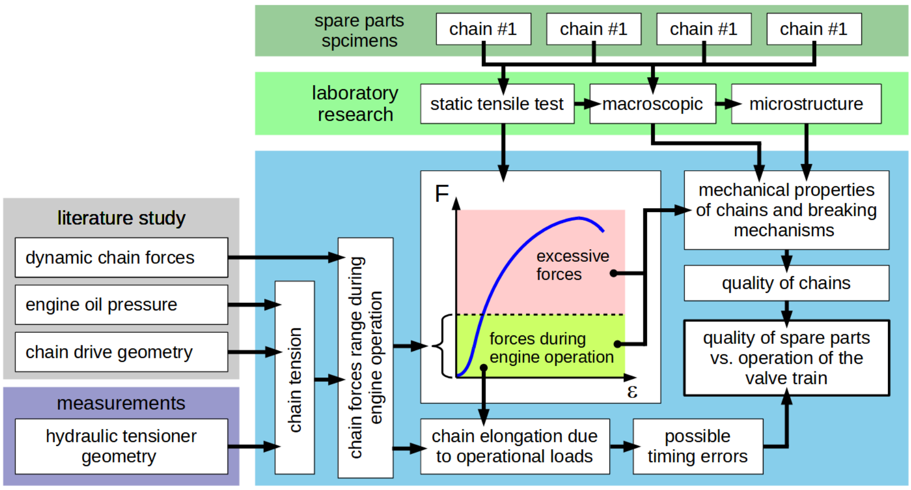

Fig. 1. Methodology and scope of chain research adopted in the work

Once the quality parameters of the tested chains were established, it was decided to estimate their influence on the operation of the timing system in an internal combustion engine. This required a range of values for the tensile forces on the chain during engine operation to be established. This was done using the results of a literature review in which the authors mathematically modeled the operation and dynamics of timing chain drives. In addition, the range of force values resulting from the operation of the hydraulic tensioner was estimated. The results were obtained from measurements of the diameter of the piston of the tensioner used, the range of oil pressures occurring during engine operation, and the geometry of the chain tensioner slides. This made it possible to determine the range of chain tension forces that could occur during engine operation. The results of the static tensile test were used to calculate the chain elongation values corresponding to these forces. Potential timing errors were then calculated from the calculated chain elongation values. Once the results of the quality tests had been taken into account, their effect on the operation of the valve train was estimated.

3. RESEARCH AND RESULTS

Four timing chains from different manufacturers were selected for testing. They were all the same size (5/16") and were single-row roller chains, type 05B-1. They differed in manufacturing details and manufacturer markings. The tested chains are shown in Fig. 2. Chain #1, shown in Fig. 2a, had the designation T027C stamped on one of the plates. Chain #2 (Fig. 2b) was marked SL 14.06. Both chains were delivered dry and clean. The sample referred to as chain #3 had the designation 05CA stamped on several plates on either side (Fig. 2c). Upon removal from the packaging, a small amount of transport grease was visible on the chain. One surprise was the condition of the last of the chains (chain #4). When unpacked, it had a lot of dirt on it, and some of its parts showed signs of corrosion. It also differed from the other three regarding the appearance of its rivet heads. An embossed JWiS marking was found on it (Fig. 2d).

Static tensile tests were carried out on a tensile testing machine, for which clamps were designed and manufactured to hold the chain safely and securely. The timing chain used was taken from the 1.3 Multijet engine. A view of the mounted timing chain prepared for testing is shown in Fig. 3a. Due to the possibility of violent breakage of the chain during fracture, a cover was also made to protect the operator from possible splinters from the broken chain (Fig. 3b).

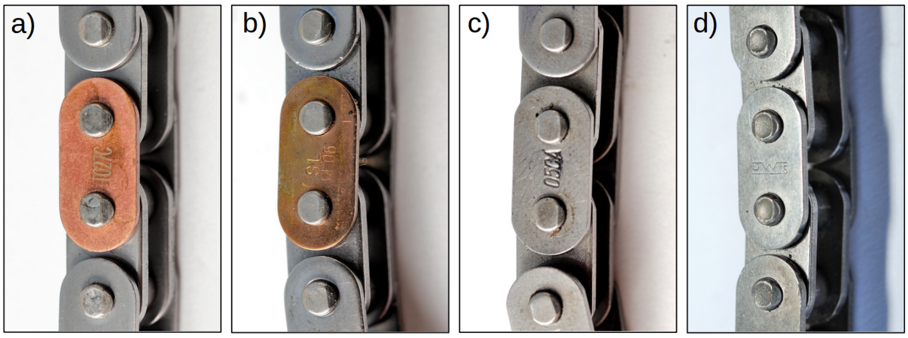

Fig. 2. Tested chains of timing system drive: a) chain #1, b) chain #2, c) chain #3, and d) chain #4

During the tests, the force was applied to the axle of the wheel mounted on the bearing so that it was evenly distributed on both branches of the tested chain loop (Fig. 3c). Therefore, the actual force in the chain is twice as low (equation 1) than the result recorded by the machine. Therefore, it will be referred to as F_C in the rest of the paper.

$$F_{C1} = F_{C2} = \frac{F}{2} \tag{1}$$

where: F_{C1}, F_{C2} – forces occurring in a single branch of the chain,
F – the force applied to the tension pulleys.

The strains of the chains were calculated (Fig. 3d) based on the deformation results obtained from Equation 2 during the tests.

$$\varepsilon = \frac{\Delta \mathrm{L}}{\mathrm{L}_0} \cdot 100\% \tag{2}$$

where: ε – strain [%],
ΔL – displacement of the tension wheel axis,
L_0 – Initial length of the stretched chain sections.

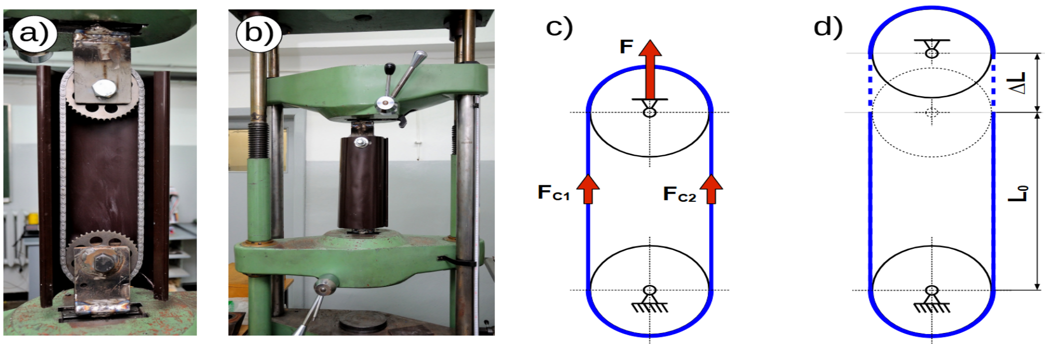

Fig. 3. Static tensile test of timing chains: a) method of chain mounting, b) view of the machine with the protective cover in place, c) distribution of forces during tests, and d) chain extension scheme

The force-strain curves obtained from the tests are shown in Fig. 4a. Based on this, Equation 3 gives the value of the elongation ratio under load, K, which indicates the elongation per kN of tensile force on the chain.

$$K_i = \frac{\varepsilon_i}{F_i} \quad \left[\frac{\%}{\text{kN}}\right] \tag{3}$$

where: K_i – coefficient of strain under specific load,
e_i – chain strain at specific load,
F_i – specific load force.

This is because the value of K is used to compare chains, which are generally required to have the smallest possible deformation. Since the values of this coefficient change as force increases, four characteristic points were chosen to compare the quality of the chains. Two forces were chosen from the range of forces that occur in the engine during operation: 0.5 kN and 1 kN. The maximum chain tensile force, F_m, and the limit force, F_L, corresponding to the turning point of the curve above which the samples deform at an increasingly faster rate, were also used for comparison. Accordingly, the values of the coefficients $K_{0.5}$, K_1, K_L, and K_m were calculated (Fig. 4b).

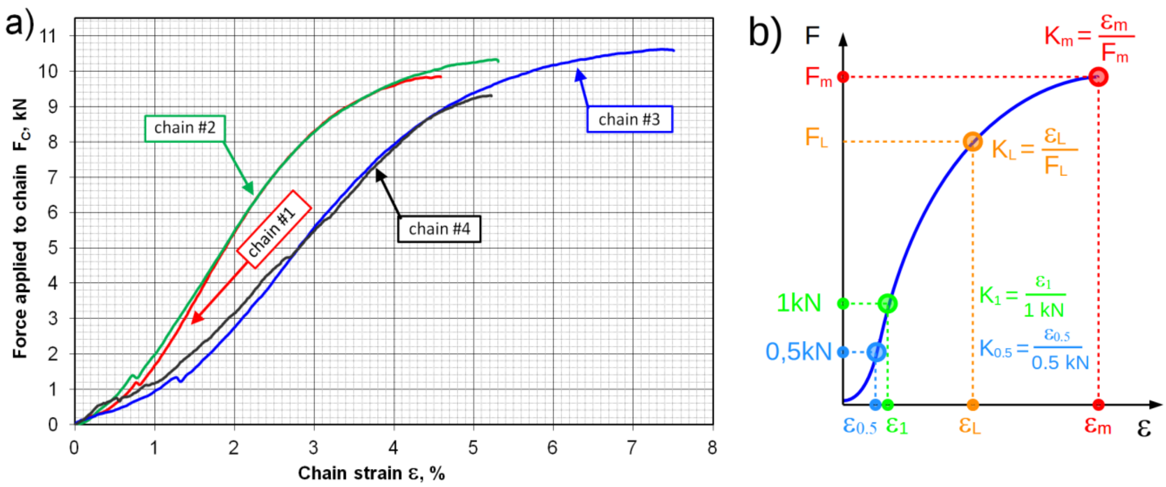

Fig. 4. a) Summary of mechanical properties of examined chains and b) scheme for determining K coefficients

To evaluate the quality of the chains, it is also useful to compare their material properties. To determine the tensile strength Rm, it was necessary to convert the force values into stresses in the material. To do this, it is important to determine the cross-sectional area of the force-transmitting material. This was done by analyzing the geometry of the chain elements and measuring their dimensions. The link plates are responsible for transmitting the longitudinal forces. The outer plates are 1 mm thick, and the inner plates are 1.5 mm thick. After the sizes of the holes for the rivets and bushes were taken into account, the areas of the active cross sections were calculated (Figs. 5a and 5b). The analysis showed that the inner plate links had the smallest active cross-sections. Therefore, this section was used for the stress and tensile strength calculations.

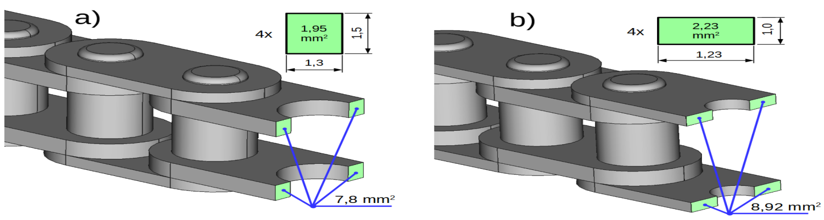

Fig. 5. Active cross-sectional area of chain links from a) inner plates and b) outer plates

In addition, for the high force range, property reserve factors were calculated between the limit and maximum values, defined for both stress (Formula 4) and strain (Formula 5). They provide information on the strength and strain reserve between reaching the limit state and chain failure.

$$r_\sigma = \frac{\sigma_{\mathrm{m}}}{\sigma_{\mathrm{L}}} = \frac{R_{\mathrm{m}}}{\sigma_{\mathrm{L}}} \tag{4}$$

where: r_σ – strength reserve coefficient,
σ_m – maximal stress = R_m – ultimate tensile strength,
σ_L – limit stress,

$$r_\varepsilon = \frac{\varepsilon_{\mathrm{m}}}{\varepsilon_{\mathrm{L}}} \tag{5}$$

where: r_ε – strain reserve coefficient,
R_m – ultimate tensile strength,
σ_L – limit stress.

The calculated values of the K and r coefficients are shown in Fig. 6. The data has been arranged and formatted to best show the differences in quality between the chains. From Fig. 6, it can be seen that, mechanically, chains #1 and #2 have the best quality, with chain #2 having the highest quality. If only the values of the K coefficients are taken as a criterion, chain #3 shows the highest deformation, which is very undesirable in an engine. Chain #4, on the other hand, has the lowest strength properties and the least strength reserve when the limit force is exceeded.

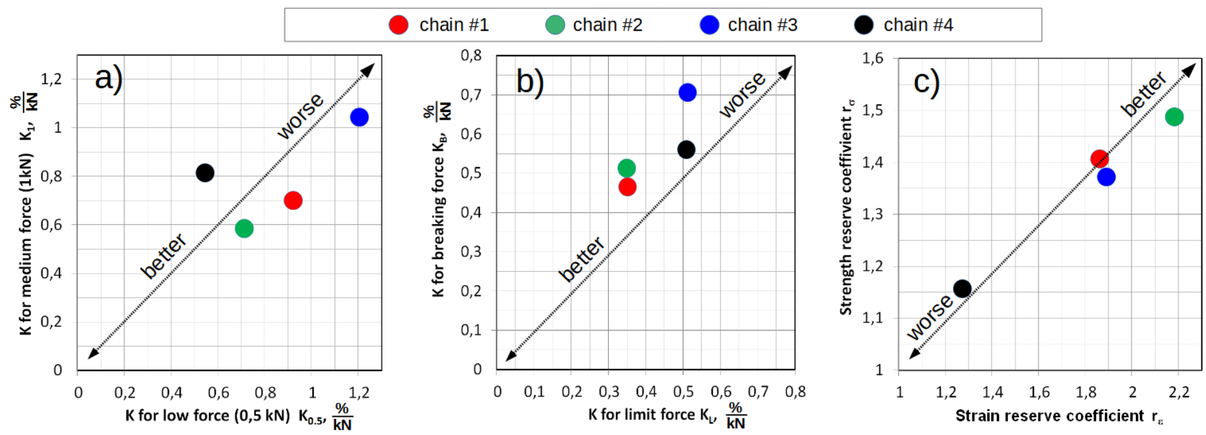

Fig. 6. Comparison of mechanical test results as indicators of chain quality for a) the range of forces occurring during engine operation, b) the range of plastic deformation, and (c) material reserve factors

The observed mechanisms of chain breakage may also indicate chain quality. A macroscopic examination of the chains was carried out after the static tensile test in order to clarify these mechanisms and the phenomena associated with fracture. Theoretical predictions and the results of the analysis of the geometry of the chain elements indicated that breakage should occur at the location of the smallest active cross-section of the tensile elements. As previously shown in Fig. 5, such locations exist within the inner plates. The assumed fracture mechanism is shown in Fig. 7a. This mechanism occurred for chains #2 and #4 as can be seen in Figs. 7b and 7c.

The mechanism of destruction of chains #1 and #3 appeared to be slightly more complicated. They failed due to damage to the rivet heads and the deformation and tearing of the outer plate holes. The mechanism of such damage is illustrated in Fig. 8a. Here, the weakest link appeared to be the riveted joint within the outer plate. As a result of the different points of application of force from the outer and inner plates and the presence of the necessary small clearances between the roller and the rivet, which is the axis of its rotation, deformation of the rivet occurs in the head area. There is also plastic deformation of the plate inside the eye, the end of which is also bent outwards. As a result, parts of the rivet head are sheared off, and the eye of the outer plate is torn. A view of the chains on which these phenomena occurred is shown in Figs. 7b and 8c.

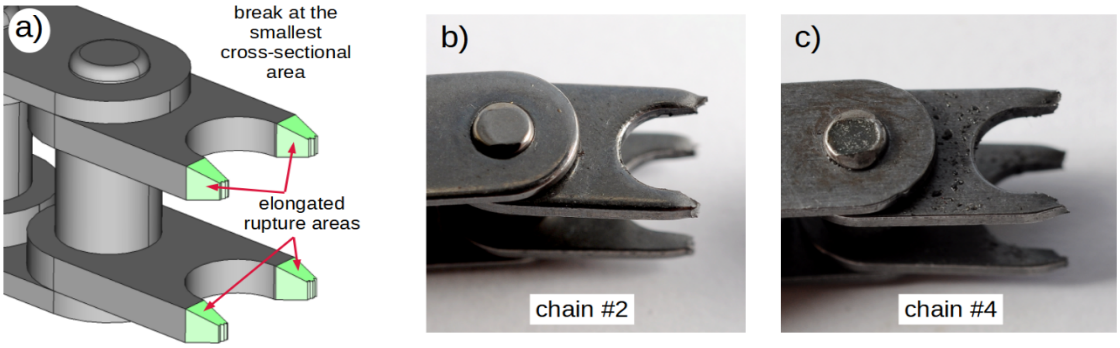

Fig. 7. Chain breakage: a) assumed mechanism, b) view of broken chain #2, and c) view of broken chain #4

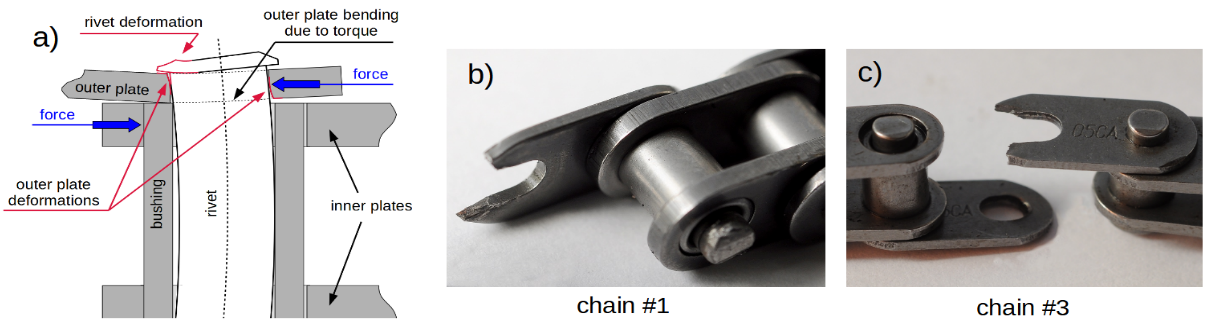

Fig. 8. Chain breakage within the outer plates: a) mechanism of the phenomenon, b) view of broken chain #1, and c) view of broken chain #3

Samples of the examined chains were also subjected to metallographic analyses to observe and evaluate the structure of the material. The tests were carried out on nitride-etched metallographic specimens using a Neophot 32 microscope. The presence of a tempered martensite structure was observed in the plates from links of chains #1, #2, and #3. This is a high-strength component and is characterized by a small range of plastic deformation. The plates of link #4 were characterized by a structure of tempered martensite and bainite, which may explain their slightly lower tensile strength. A microscopic examination of the rivets of the chains studied revealed a greater variety of structure. In the case of chain #1, this was tempered martensite. Chain #2 rivets have a mixed structure of tempered martensite and bainite. In contrast, the rivets of chains #3 and #4 have a structure of tempered bainite with inclusions of ferrite. This structure may be characterized by higher plastic deformability, as ferrite is a soft and ductile component.

In order to comprehensively assess the quality of the chains, a parametric multi-criteria evaluation was proposed. Selected parameters and characteristics of the tested chains were collected and for each of them a score was calculated or assigned in the range 0...1. If the parameter under consideration was characterized by a numerical value, it was normalized according to Formula 6.

$$q_n = \frac{n - n_{\min}}{n_{\max} - n_{\min}} \tag{6}$$

where: q_n – quality score for parameter n for specific chain,
n – value of parameter n for specific chain,
n_{min} – minimum value of the n parameter among all timing chains,
n_{max} – maximum value of the n parameter among all timing chains.

If an increase in the value of a parameter led to a decrease in quality (e.g., elongation), an adjustment was made according to Formula 7.

$$q_n' = 1 - q_n \tag{7}$$

where: q_n' – reversed quality score for parameter n for a specific chain.

Parameters of a non-numerical nature, such as structure or breaking mechanisms, were manually assigned quality score values. The quality scores calculated in this way are summarised in Table 1, at the end of which all q_n indicators are summarized. The Q_i value calculated in this way forms the basis for a comprehensive and multi-criteria evaluation of the quality of commercially available spare parts.

Table 1

Analysis of quality indicators for tested timing chains

	Parameter value				Normalized quality score for tested chain q_n			
Parameter	chain #1	chain #2	chain #3	chain #4	#1	#2	#3	#4
R_m	1263.82	1325.64	1361.54	1194.59	0.41	0.78	1.00	0.00
σ_m	4.50	5.31	7.51	5.21	1.00	0.73	0.00	0.76
$K_{0.5}$	0.92	0.71	1.21	0.55	0.43	0.75	0.00	1.00
K_1	0.70	0.58	1.04	0.81	0.75	1.00	0.00	0.50
K_L	0.35	0.35	0.51	0.51	0.99	1.00	0.00	0.02
K_m	0.47	0.51	0.71	0.56	1.00	0.80	0.00	0.61
r_σ	1.41	1.49	1.37	1.16	0.76	1.00	0.65	0.00
r_ε	1.86	2.18	1.89	1.27	0.65	1.00	0.68	0.00
link microstructure	tempered martensite	tempered martensite	tempered martensite	tempered martensite + bainite	1.00	1.00	1.00	0.50
rivet microstructure	tempered martensite	tempered martensite + bainite	tempered bainite + ferrite	tempered bainite + ferrite	1.00	0.50	0.00	0.00
breakage mechanism	rivet head	inner plate	rivet head	inner plate	0.00	1.00	0.00	1.00
delivery condition	clean, dry	clean, dry	grease	dirt, rust	1.00	1.00	0.50	0.00
summary quality score Q_i					**9.0**	**10.6**	**3.8**	**4.4**

Based on the analysis of the Qi values, it can be stated that chain #2 has the highest quality, with a score of 10.6. Chain #1 ranks second, with a slightly lower value of 9.0. The quality of chain #4 was much lower, with a Qi value of only 4.4. Chain #3 had the lowest Qi value of 3.8.

4. CHAIN ELONGATION VS. TIMING ERROR

During the operation of an internal combustion engine, the timing chain is subjected to variable tensile forces. These come from the power transmitted between the crankshaft and the camshaft as well as from the chain tensioning system, which ensures that the chain is correctly guided. The Multijet 1.3 engine uses a hydraulic tensioner with a lever fitted with a sliding chain guide element. The operating principle of the tensioner is shown in Fig. 9a.

To determine the range of forces that can be transmitted by the tensioner, the diameter of its piston was measured. It has a diameter of D = 15 mm, giving a cross-sectional area of S = 176.6 mm^2. The engine oil pressure acts on the piston surface to produce the force Fh. According to the engine documentation, its minimum value for idling is 0.08 MPa. The maximum oil pressure in the engine (0.45 MPa) is limited by the opening of the oil pump bypass valve. The tensioner piston acts on the lever with the slide at a distance of L_1 = 182 mm from its axis of rotation. By changing the curvature of the sliding element of the guide, the force from the tensioner is applied to the chain at a distance of L_2 = 216 mm from the axis of rotation (Fig. 9b). Its value F_h' can be calculated using Equation 8.

$$F_h' = F_h \cdot \frac{L_1}{L_2} = p \cdot S \cdot \frac{L_1}{L_2} \tag{8}$$

The relevant geometry parameters of the tensioning system components were then determined (Fig. 9c), including the angle of force application from the tensioning lever a = 117.6^{O}. This made it possible to estimate the value of the chain tensioning force F_C, calculated by Equation 9.

$$F_C = \frac{F_h'}{\sin\gamma} = \frac{F_h'}{\sin(\alpha - 90^{O})} \tag{9}$$

Using the above relationships, chain tension force values were calculated for the oil pressures that can occur in the engine (Fig. 9d). These forces range from approximately 25 N to just under 150 N. It should be noted that this estimate does not take into account small changes in angle resulting from a possible change in the position of the lever with the guide bar. This simplification was due to the need to establish a range of possible forces rather than specific values.

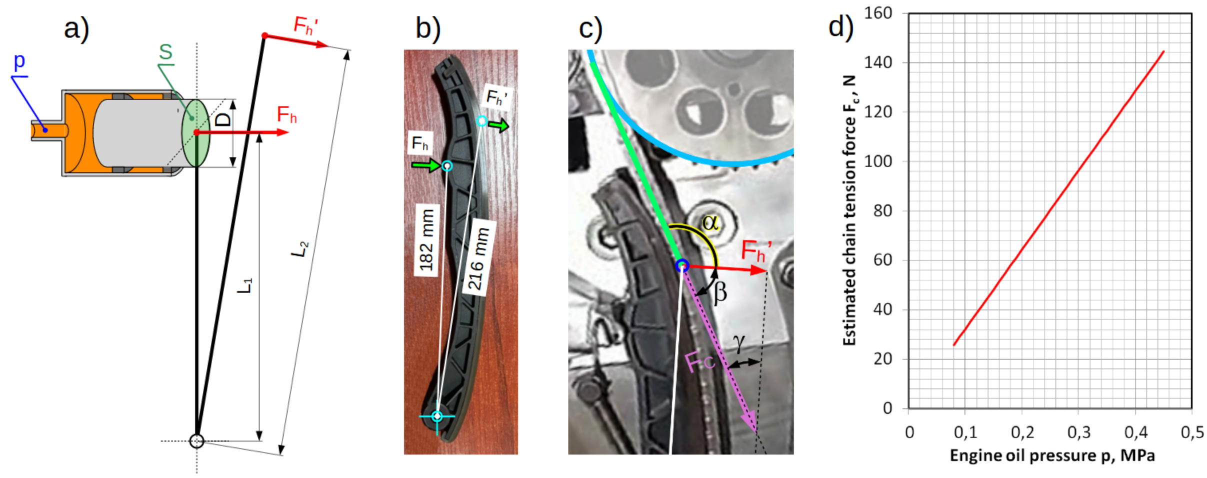

Fig. 9. Hydraulic timing chain tensioner: a) operating principle b) tensioner lever geometry, c) relative position of chain and tensioner lever, and d) diagram of chain tensioning force vs. engine oil pressure

The operation of the timing system is characterized by high dynamics and the occurrence of variable tensile forces on the chain, as confirmed by the results of many published experimental studies and mathematical modeling. The results of the mechanical properties of the chains presented in Chapter 3 show that the tested chains stretched when forces were applied. They broke when subjected to high tensile forces. According to the literature analysis presented in Chapter 1, during the operation of engines with a similar valve train design to the Multijet 1.3, forces with maximum values in the range of 1–1.2 kN can be expected [8, 10, 12, 14]. As can be seen, the range of maximum dynamic forces is approximately 10 times greater than that of the hydraulic tensioning system. These are well below the tensile strength of the chain and are in the range of approximately 10–13% of the breaking load. However, the characteristics shown in Fig. 3 indicate that all tested chains also elongate in the low force range.

Taking into consideration the relatively low values of the forces in relation to the tensile strength, it is most likely that these are elastic deformations of the chain components. The question then arises as to whether these elongations can affect the operation of the timing system and, in particular, the precision of the camshaft phasing. In order to answer this question, it must be taken into account that the tested chains were mounted in a slightly different configuration during stretching than in the engine. In order for the two branches of the chain to run in parallel, they were mounted on two identical sprockets from the engine camshaft (Fig. 10a). These have 42 teeth each.

Consequently, their banding angle is 180 degrees, and the chain rests on half of the sprockets (i.e., 21 teeth each). Because the links are supported on the teeth of the sprockets, these sections of the chain cannot stretch. As the tested chains had 120 links, the remaining 78 links, divided into two sections of 39 links each, were subjected to stretching.

The timing chain in the engine is located between wheels of different sizes and is additionally guided by curved sliding guides (Fig. 10b), one of which acts as a hydraulic tensioner. The drive sprocket is located on the crankshaft and has 21 teeth. To maintain the correct 1:2 ratio, the camshaft sprocket has 42 teeth. Observations on the engine revealed that the chain is supported by 26 teeth of the larger sprocket and 12 teeth of the smaller sprocket. This gives wrap angles of 222.9 degrees at the camshaft and 205.7 degrees at the crankshaft. Between the wheels, there are two sections of chain, each 41 links long. As the crankshaft transmits the drive to the camshaft, only one of the chain sections is subject to high tension.

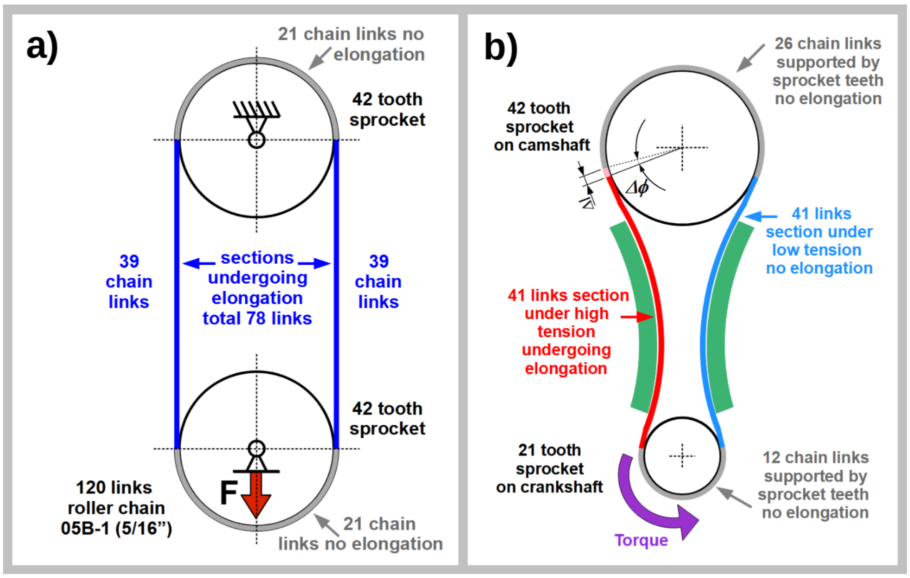

Fig. 10. Diagrams showing the stretched sections of timing chains mounted on a) the test bench and b) the engine during operation

In the theoretical ideal situation, if the chain were not stretched, there would be one camshaft revolution for every two crankshaft revolutions. However, if the camshaft is subjected to heavy resisting forces and there is a significant amount of tension on the active part of the chain, it will stretch and the camshaft rotation will be reduced by a certain small angle due to the elongation of the chain. In order to assess how much variation in camshaft angle could be experienced by the chains tested on the Multijet 1.3 engine, the elongation characteristics were converted to camshaft angle Based on the results obtained from the static tensile test according to Formula 10, the ΔL_M elongation of the 41-link engine-mounted chain section was calculated for each measuring point:

$$\Delta L_M = \frac{\varepsilon_i}{100\%} \cdot L_{41} = \frac{\varepsilon_i}{100\%} \cdot 41 \cdot (5/16)" \qquad (10)$$

where: ε_i – strain for the chosen force F_i,
L_{41} – length of 41 link chain section.

The angle of rotation of the camshaft corresponding to the calculated chain elongation was calculated considering that the elongation of the chain by one link length (pitch) corresponds to the angle of rotation of the sprocket by one tooth, while the elongation of the chain can be expressed as a fraction of its pitch length. This angle has been calculated using Relation 11.

$$\Delta\phi = \frac{\Delta L_M}{p} \cdot \frac{360^O}{z_C} = \frac{\Delta L_M}{(5/16)"} \cdot \frac{360^O}{42} \qquad (11)$$

where: p – chain pitch = 5/16”,
z_C – number of teeth on the camshaft sprocket = 42.

The calculated values of the camshaft rotation angles corresponding to the elongation of the tested timing chains if they had been installed in the engine are shown in Fig. 11.

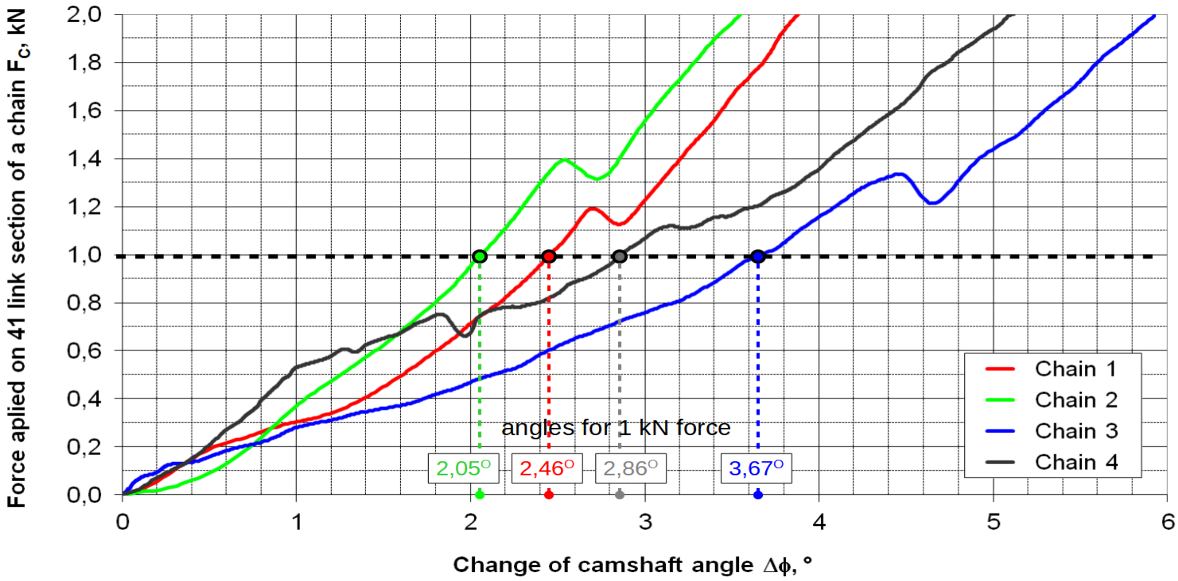

Fig. 11. Camshaft phasing inaccuracy as a result of chain stretching depending on chain tensile force

Fig. 15 shows that, for average forces occurring during timing system operation of several hundred N, chain stretching will result in a camshaft phase shift of approximately 1 degree. However, at maximum forces of around 1 kN, the phase shift for most of the tested chains is between 2 and 2.9 degrees. Chain 3 shows much higher deformations, and for this chain, the camshaft phase shift will be as high as 3.7 degrees.

In addition, it should be noted that the characteristics of all the tested chains show noticeable non-linearities, which manifest themselves in a ripple pattern. This is a typical sign of plastic deformation. Chains #1, #2, and #3 show such an irregularity in the range of 1.2–1.4 kN. Chain #4, on the other hand, stretched more unevenly, and its characteristics show several permanent elongations in the range of 0.6–1.1 kN. This is not a good indication of its quality, although it can be compensated for by the hydraulic tensioning system when the engine is running.

The results of the calculations confirm that the use of chain #2 in the engine, which had the best quality parameters among the samples tested, will be the most advantageous since it will cause the fewest camshaft positioning errors. The order of the results obtained from best to worst corresponds to the order of the Q_i quality indicators calculated in Chapter 3.

5. CONCLUSIONS

The results of this research confirm that commercially available spare parts in the form of timing chains for the 1.3 Multijet engine are characterized by different properties as well as strength and performance parameters. Therefore, it is important to develop as objective a system as possible for evaluating the quality of spare parts so that automotive service companies can use it as a guide when planning the stocking of their warehouses.

The multi-criteria parametric method for evaluating the quality of timing chains proposed in this study can successfully form the basis for further development work and possible implementation. It is largely based on the results of a static tensile test. This test provides insights into the force-strain characteristics of the evaluated timing chains. Thus, in addition to determining the tensile strength or maximum deformation of the material, it is possible to determine a variety of numerical coefficients that describe the behavior of the chain not only in the high breaking force range but also in the low and medium force range. This is important because the forces involved are usually no more than 10-13% of the chain strength. The proposed multi-criteria parametric chain quality evaluation system was complemented by an evaluation of the material microstructure of the chain-forming elements, as this also affects the mechanical parameters of the chains. The most favorable structure was tempered martensite. The least favorable structure was bainite with soft ferrite inclusions. As part of the quality assessment system, chain fracture mechanisms were also investigated. The quality of the chains was described by coefficients Q_i, which is the sum of all unit factors q_n considered.

The research shows that the tested timing chains broke at forces of 9.3 and 10.6 kN, giving a calculated tensile strength in the range of approximately 1200...1360 MPa.

Breakage can occur at the point of the smallest active section of the chain. The second possibility is the shearing of the rivet head with subsequent deformation or fracture of the outer plates within the hole. Significant differences in chain elongation were also recorded, ranging from 4.5–7.5%. The recorded tensile characteristics of the chains show that at forces above 1.2–1.3 kN, the chains begin to show signs of permanent elongation. Against this background, the characteristics of chain #4 were much worse, being much less homogeneous and showing the first signs of permanent elongation at forces as low as 0.7 kN.

The calculations carried out in the paper, based on the geometry of the timing chain tensioning system, made it possible to estimate the range of values of the tensile forces generated by the hydraulic tensioner. This range starts at 25 N and ends at around 150 N, which is just over 10% of the estimated dynamic forces resulting from the operation of the timing system.

This study also estimated inaccuracies in the camshaft angle setting due to elastic elongation of the chain under the forces encountered during engine operation. For the chains studied on the Multijet 1.3 engine, these displacements can be in the order of 1 degree in the medium force range. However, at maximum dynamic forces in the range of 1 kN, the camshaft phasing inaccuracy increases to around 2–3.7 degrees, which is already a value that should be taken into account when designing the engine timing system.

The results of the multi-criteria parametric chain quality evaluation system were confirmed by the results of the estimation of camshaft position errors resulting from chain stretching due to forces occurring during engine operation. The order of results from the quality evaluation system started with the best chain (i.e., chain #2), which scored 10.6 points, followed by the next best chain (chain #1; 9.0 points) and the next to last chain (chain #4; 4.4 points). Chain #3 had the lowest quality score (3.8 points). This order coincides with the results of the camshaft position errors and confirms the validity of the criteria used to assess quality. Such a system can be further modified and extended, for example, by adding additional weighting factors to differentiate the influence of each parameter on the overall score.

References

1. Michlberger, A. & Sutton, M. LSPI durability, a study of LSPI over the life of a vehicle. *SAE International Journal of Engines.* 2018. Vol. 11. No. 1. P. 23-38.
2. Maile, K. & Campean, F. & Day, A. Design for reliability of an engine timing chain. *SAE Technical Paper.* 2009. No. 2009-01-0206. P. 1-10.
3. Domek, G. Design trends in timing belts. *Scientific Journal of Silesian University of Technology. Series Transport.* 2014. Vol. 1. P. 59-66.
4. Gagg, J. A Friction comparison between chain and belt-drive systems. *SAE Int. J. Engines.* 2012. Vol. 5. No. 2. P. 353-362.
5. Hyakutakea, T. & Inagakia, M. & Matsudaa, M. & Hakamadaa, N. & Teramachib, Y. Measurement of friction in timing chain. *JSAE Review*. 2001. Vol. 22. P. 343-347.
6. Howlett, M. & Ausserhofer, N. & Schoeffmann, W. & Truffinet, C. & Zurk, A. Chain versus belt – system comparison of future timing drives. *International Journal of Automotive Engineering.* 2016. Vol. 7. P. 135-141.

7. Sauer, B. & Krupp, F. & Becker, A. Power loss reduction in timing chain drives by adjusted tensioning and surface structuring. *Industrial Lubrication and Tribology*. 2019. Vol. 71. No. 8. P. 997-1002.
8. Chen, Y. Dynamic analysis and structure improvement of timing chain of an engine. *Journal of Physics: Conference Series.* 2020. Vol. 1699. P. 1-7.
9. Xi, J. & Feng, Z. & Wang, G. & Guo, H. Kinetic and dynamic characteristics analysis of timing chain system for diesel engine. *Applied Mechanics and Materials*. 2014. Vol. 602-605. P. 398-403.
10. Mulik, A.V. &, Gujar, A.J. Literature review on simulation and analysis of timing chain of an automotive engine. *International Journal of Engineering Research and Application.* 2016, Vol. 6. No. 8. P. 17-21.
11. Mulik, R.V. & Joshi, M.M. & Gajjal, S.Y. & Ramdasi, S.S. & Marathe, N.V. Dynamic analysis of timing chain system of a high speed three cylinder diesel engine. *International Journal of Engineering And Science.* 2014. Vol. 4. No. 5. P. 21-25.
12. Yang, J. & Feng, Z. & Gao, H. & Wang, T. & Xu, K. Multibody dynamics analysis of a silent chain drive timing system. *Journal of Mechanical Science and Technology*. 2023. Vol. 37. No. 4. P. 1653-1664.
13. Cali, M. & Sequenzia, G. & Oliveri, S.M. Meshing angles evaluation of silent chain drive by numerical analysis and experimental test. *Meccanica*. 2016. Vol. 51. P. 475-489.
14. Xi, J. & Liu, N. Research about vibration characteristics of timing chain system based on short-time Fourier transform. *IOP Conf. Series: Materials Science and Engineering.* 2017. Vol. 231. P. 1-5.
15. Feng, Z. & Yang, J. & Wang, F. Dynamic simulation and test verification of hydraulic automatic tensioner for an engine timing chain drive system. *Chinese Journal of Mechanical Engineering.* 2023. Vol. 36. No. 122. P. 1-13.
16. Becker, A. & Meffert, D. Sauer, B. Friction and wear investigations on single chain joints. *Forsch Ingenieurwes.* 2019. Vol. 83. P. 53-63.
17. Tandler, R. & Bohn, N. & Gabbert U. & Woschke, E. Analytical wear model and its application for the wear simulation in automotive bush chain drive systems. *Wear.* 2020. Vol. 446-447. P. 1-9.
18. Paulovics, L. Timing chain wear investigation methods – review. *FME Transactions*. 2022. Vol. 50. P. 461-472.
19. Jung, T. & Park, Y. & Kim, Y.J. & Cho, Ch. Integrated approach to an optimal automotive timing chain system design. *International Journal of Automotive Technology*. 2017. Vol. 18. Issue. 6. P. 1037-1045.
20. Kumar, J.S. & Giridharan, S. & Kannan, T.T.M. & Kumar, P.V. Study and overview about process failure mode and effects analysis on automotive timing chain. *International Journal of Research in Mechanical Engineering*. 2014. Vol. 2. No. 5. P. 17-21.
21. Zhou, Y. Mathematical modeling of chain drive geometries for a durability test rig. *Experimental Techniques*. 2015. Vol. 40. P. 1137-1146.
22. Filipczyk, J. Causes of automotive turbocharger faults. *Transport Problems*. 2013. Vol. 8. No. 2. P. 5-10.
23. Schöffmann, W. & Howlett, M. & Truffinet, C. et al. Future timing drives chain and belt in competition. *MTZ Worldwide.* 2015. Vol. 76. No. 7. P. 20-25.
24. Sauer, B. & Nicola, A. & Flierl, R. et al. Features of timing chain drives. Integration of experiment and dynamics simulation. *MTZ Worldwide.* 2007. Vol. 68. No. 12. P. 28-30.

Received 12.05.2023; accepted in revised form 27.11.2024